



Petrographical and petrophysical properties of the Upper Cretaceous Matulla Formation at Gabal Libni, Sinai, Egypt

Abuseda, H.^{1*}, Nabawy, B. S.², Kassab, M.³ and El-Sawy, M.³

¹Production Department, Egyptian Petroleum Research Institute (EPRI), 11727, Cairo, Egypt

²Department of Geophysical Sciences, National Research Centre, Cairo, Egypt

³Exploration Department, Egyptian Petroleum Research Institute (EPRI), 11727, Cairo, Egypt

Corresponding author: heshamabuseda@epri.sci.eg & heshamabuseda@yahoo.com

Abstract

The present work aims to flash up at the microfacies and integration of reservoir properties of 86 core limestone samples collected from Matulla Formation (Upper Cretaceous) at Gabal Libni were collected. The studied Matulla Formation is classified into five types of microfacies: Dolostone, Echinoidal foraminiferal grainstone, Echinoidal foraminiferal packstone, Echinoidal bioclastic packstone/grainstone, and Molluscan echinoidal packstone, the studied samples reveals most of the carbonate samples were tight, and various diagenetic processes including Dolomitization, Neomorphism, and Dissolution with iron oxides, carbonates, or clays. The porosity of rock samples directly affects the bulk density, as it increases if the porosity is filled by oxides (iron oxide) or cemented by clay content (cementation). The limestone reservoir reflects poor characteristics in most intervals as a result of low porosity and low permeability due to matrix and diagenesis. The reservoir quality index (*RQI*) is controlled mainly by permeability and the reservoir quality of carbonate rock samples are very low. The *FZI* for all carbonate microfacies ranged from 0.06 to 1.91 μm which infers impervious to poor reservoir quality. The pore throat radius R_{35} ranges from 0.01 to 2.66 μm , comprised of micro-mesoporosity $0.01 \mu\text{m} < R_{35} \leq 2 \mu\text{m}$, due to their tight nature, are generally impervious to poor flow potential and the studied carbonate microfacies are expressed by two hydraulic flow units.

Article Info

Received 3 Mar. 2022.

Revised 3 Jul. 2022.

Accepted 14 Aug. 2022.

Keywords

Matulla Formation,
 reservoir quality index,
 hydraulic flow units

Introduction

Petrophysical properties such as porosity and permeability of reservoir control the flow of fluids in the pore space and storage and therefore the production of oil, water, or gas reservoirs. Both permeability and porosity can be easily determined. Permeability is described by Darcy's law for the flow of fluids in porous media. The permeability may be affected by many factors such as rock porosity, grain shape, grain size, texture, cementation, and space geometry. The pores are interconnected, and the pore throats are large enough to permit the flow of fluids. A pore network is made up of larger spaces that are referred to as pores, which are connected by small spaces referred to as pore throats. In other hand, the pore space volume is reflected by the porosity, while

the pore throats is reflected by the permeability of a rock. The geometric relationship between pore throats and pore spaces controls the relation between permeability and porosity. The relation between permeability and porosity studied by many authors, e.g., [1, 2, 3, 4, 5, 6, and 7]. Many authors used HFUs for permeability modeling and rock typing (e.g., [8 and 9]). For the analysis of hydraulic flow units (HFU) were provided core analysis data [10]. In the present work collected 86 samples from Matulla Formation lies in Gabal Libni located in the North Sinai folds which represent Late Cretaceous and this work aims to flash up at the microfacies and reservoir properties, the petrographical studies aim to describe the various litho-facies with emphasis on detrital mineralogical composition, rock textures, and materials of cementation to determine the prevailed conditions to

interpret the paleo-environment during the deposition these sediments, and the study of petrophysical is mainly devoted to analyzing core samples recovered from Matulla Formation (Upper Cretaceous) for studying the effects of rock properties, reservoir quality index, flow zone indicator, and flow capacity.

Geological settings

Sinai Peninsula is one of the several semi-independent blocks in the eastern Mediterranean Sea that interacting with other plates, for the hydrocarbon production enhancement and development, its area covers about 60,000 km² approximately. Gradually, the dips of the area from northward to the Mediterranean Sea. It has a triangular shape pounded by Gulf of Aqaba at the east, by Gulf of Suez at the west and by the Mediterranean Sea at the north [11]. Sinai Peninsula composed of two main subdivision structure units, the stable shelf include the southern part while unstable shelf include the northern part. At the late Cretaceous, stable shelf was deformed to small structural, while the unstable shelf is divided to many trending synclines and anticlines belonged to the Syrian Arc System such as ENE-WSW [11, 12, 13, and 14]. Also, the period of late Cretaceous was represented by the global static sea-level rise and Sinai Basin formation was controlled by a part of Arabo-Nubian platform represented by wide, abroad shallow shelf of carbonate intercalated with of silica clastic [15, 16, 17, 18, and 19] managed to divide Sinai into three physiographic sections: (1) The southern part of the peninsula represented by high, rugged, and complex mountains composed of metamorphic and igneous rocks back to Precambrian basement (2) at the central tip of the peninsula, during Mesozoic and Cenozoic eras, a dissected plateau was developed consisting of sandstones, limestone and dolostone, (3) in the north there is a sandy plain that parallels the coastline. The study area as figure 1 lies in the northern sector in the unstable shelf of Sinai Peninsula between latitudes 29° 55" and 31° 30"N and longitudes 32° 35" and 34° 25"E. which is covered with a northward draining limestone plateau. During the fieldwork, the stratigraphic sequence of the Upper Cretaceous in the study area was represented by four formations arranged as: Halal formation at bas, Wata and Matulla formations in the middle and Sudr formation at the top.

Methodology

Mineralogical investigations

Total of 40 representative samples out of 86 carbonate samples were studied to analyze the microfacies present based on a polarizing microscope in the Matulla Formation (Upper Cretaceous) in Gabal

Libni. Porosity different types were distinguished by impregnated samples using blue dye [20].

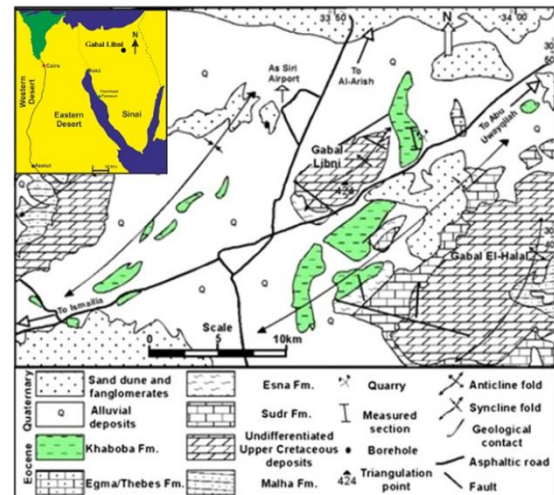


Figure. 1: Location and Geological map of Gabal Libni (modified after **Temraz 2010**).

Microfacies investigations usually elucidate the rock constituents, cement and pores, diagenesis, and depositional characteristics. In the present study, pore spaces was nomenclature and classify using classification [21]. The description of these carbonate rocks is based on the study of the present thin sections and their classification followed the schemes of [22]. The equivalent environments of the identified microfacies types were determined following [23 and 24]. Petrographically, the carbonate samples can be categorized into five different types of microfacies: Dolostone, Echinoidal foraminiferal grainstone, Echinoidal foraminiferal packstone, Echinoidal bioclastic packstone/grainstone, and Molluscan echinoidal packstone, depending on the faunal content, texture, structure, and mineralogical composition.

Petrophysical investigations

The measurements of petrophysical properties (86 core limestone samples) were determined by preparing the collecting samples as core plugs with diameter 2.55 cm and lengths 4 cm using drilling machine of a diamond cutter. The studied samples have been cleaned by a specific solvent that preserves the structure of the sample. Samples were dried to remove pore water and cleaning solvent. After constant weights had been achieved, all the samples were cooled to the room temperature in moisture-free desiccators. The analyzed samples were carried out at the laboratory of Egyptian Petroleum Research Institute (EPRI) and laboratory of National Research Centre (NRC). The petrophysical laboratory investigation was carried out and the standard parameters are calculated to determine the characterization of the reservoir, as grain density, formation factor, permeability and porosity.

Density and porosity

Density and porosity are sometimes measured as one package. The density can be classified into: a) bulk density and b) grain density. The first one (bulk

density) can define as the mass of a rock per unit volume in normal state. The density depends on solid phase (grains and cement), voids or spaces (porosity) and types of fluids saturating the pore spaces of the rock, bulk density is calculated by the following equation:

$$d_b = \frac{m}{V} \quad (1)$$

Where; d_b is the bulk density of unit g/cm^3

m is the sample mass g

V is the samples volume per unit cm^3 .

Density of grain means the grain mass only or solid grains volume (V_g), which is expressed similarly:

$$d_g = \frac{m_g}{V_g} \quad (2)$$

Where; d_g is the grain density (g/cm^3), m_g is the mass of the sample (gm), and V_g is the volume of the samples (cm^3).

Reservoir porosity is the main important factor for characterization and evaluating the capacity of reservoir represented by storage pore space.

Porosity (Φ) is defined as the pore space volume V_p divided by total rock sample volume (V):

$$\Phi = \frac{V_p}{V} \quad (3)$$

Where; Φ is the porosity, V_p is the sample pore space volume per unit cm^3 , V is the sample bulk volume per unit (cm^3).

Permeability

Permeability is defined as the rock ability to conduct fluids through a porous material, typically measured by unit of Darcies or millidarcies. It is controlled by several parameters like as geometry, texture, roundness, cementation of the rock pore and grain shape and size. Permeability was determined by using A Ruska gas permeameter and calculated by Darcy's law equation for viscous compressible fluid permeability in porous material as follows;

$$K = \frac{(2000 * \mu * q * L * P_a)}{A(P_1^2 - P_2^2)} \quad (4)$$

Which; k : is the permeability per unit mD, L is the sample length per unit cm, μ : is the gas viscosity per unit centipoises, q : is the volume flow rate of gas per unit cm^3/sec , P_a : is the normal atmospheric pressure, P_1 : is the upstream pressure, P_2 : is the downstream pressure A : is the sample cross-sectional area per unit (cm^2).

Hydraulic flow unit

Reservoir rock heterogeneity and quality were classified and divided by using the concept of hydraulic flow unit [10]. The geological properties such as pore geometrical microfacies, texture and mineralogy can be determined by calculations of the flow zone indicator (FZI) depended on the porosity and permeability values. Also, the calculations of the reservoir quality index (RQI), and normalized porosity index (NPI) depended on the porosity and permeability values:

The (RQI) and (NPI) are calculated as follows:

$$RQI = 0.0314 \sqrt{k/\Phi} \quad (5)$$

$$NPI = \frac{\Phi}{(1-\Phi)} \quad (6)$$

$$FZI = \frac{RQI}{NPI} \quad (7)$$

Formation Factor

The formation resistivity factor is a very important parameter that was discussed by many authors, such as [25, 26, 7, 27, and 28] and others. [29] first defined the property of a porous medium known as "formation resistivity factor" as:

$$\text{True formation resistivity} = \frac{\sigma_w}{\sigma_0} \quad (8)$$

With σ_0 is the rock sample resistivity and σ_w is the brine resistivity.

In the case high salinity water, represented as a good true formation factor. The results of cementation and particle size on the formation resistivity factor of different materials was analyzed by [30]. Observed formation resistivity factor for artificially cemented aggregates showed that the cemented aggregates exhibit a greater difference in porosity than the unconsolidated one. The relation between formation factor and porosity depending on cementation exponent (m) and lithology constant (a) represent lithology [29].

$$F = a\Phi^{-m} \quad (9)$$

The effective interconnected porosity is defined as the inverse value of the formation factor [31].

Results

Petrographic Investigation

A polarizing microscope was used for petrography and mineralogy investigation to examine the carbonate samples by prepared carbonate thin sections to analyze the texture and composition and discussed the petrographic classification and diagenetic history. The carbonate samples in the Matulla Formation (Upper Cretaceous) in Gabal Libni can be categorized into five different types of microfacies:

Dolostone

Dolomitic packstone microfacies was marked at the lower part of Matulla Formation which, composed of dolomitic crystals embedded in a micrite matrix (figure 2A). Dolomite crystals have euhedral to sub-hedral (idiotypic to hypidiotypic), boring, and fine to very fine texture. These crystals are occasionally zoned with iron oxide nuclei (figure 2B). Few (< 2% bioclastic grains can be observed in these microfacies and represented by pelecypod fragments that are recrystallized and formed of fibrous calcite. All components are scattered in a micrite matrix that is partially neomorphosed into dolomite crystals. Porosity is represented by Vug (figure 2A), intercrystalline, and intracrystalline (figure 2C) porosity types. The dissolution of dolomite crystals is well developed in this microfacies owing to forming of intracrystalline porosity. The enrichment of the micrite matrix and the depletion of the bioclastic grains, with exception of a few pelecypod, reflect the deposition of this microfacies in a quiet, restricted shallow subtidal environment. This interpretation of

depositional environment matches with that of [23] to his FZ7 microfacies.

Echinoidal foraminiferal grainstone

Echinoidal foraminiferal grainstone microfacies was located at the middle part of the studied Matulla Formation. Echinoid fragments as well as foraminiferal tests and pelecypod shall fragment to form about 60% of the rock. Echinoid fragments are of fine size with overgrowth calcite cement. Foraminiferal tests are filled by micrite matrix while their walls are recrystallized into calcite sprite. Pelecypod shall fragment are made up of fibrous calcite that is occasionally recrystallized into macrocrystalline mosaic calcite crystals. Allochems are embedded in crystalline calcite cement with relics of calcite matrix that reveal the neomorphism of cryptocrystalline calcite matrix to macrocrystalline calcite cement. The porosity of this microfacies is represented by intercrystalline, channel (figure 2D), and vug (figure 2E) porosity types. The high diversity of the bioclastic grains in this microfacies as well as the initial cryptocrystalline calcite matrix can be reflected quiet open marine, platform interior below fair-weather wave base with low circulation conditions that coincides with the microfacies types (FZ7) of [23].

Echinoidal foraminiferal packstone

Echinoidal foraminiferal packstone microfacies type is detected at the middle part of the Matulla Formation. Allochems are represented by echinoid fragments as well as few foraminiferal tests and pelecypod shall fragments to form about 40% of the rock. Echinoid fragments are of fine to very fine size with overgrowth calcite cement. Foraminiferal tests are filled by micrite matrix (figure 2F) while their walls are recrystallized into calcite sprite. Pelecypod shall fragments are made up of fibrous calcite that is occasionally recrystallized into macrocrystalline mosaic calcite crystals. These allochems are embedded in the cryptocrystalline calcite matrix. Porosity is less than the former microfacies and is represented by vug and intercrystalline (figure 2G) porosity types. The predominance of mud-supported textures, the diverse faunal association content, and the absence of terrigenous influx suggest a deeper open-marine platform interior environment with open circulation, normally above fair-weather wave base [24].

Echinoidal bioclastic packstone/grainstone

This carbonate microfacies type was found at the middle part of the studied section. Allochems compose ranged from 30 to 40 % of the rock and are represented by echinoids well as a few (5%) pelecypod fragments. Echinoid fragments are characterized by overgrowth calcite cement, while the pelecypod shall fragments recrystallized into prismatic macrocrystalline calcite. The allochems are embedded in a micrite matrix that is partially recrystallized into micro – macrocrystalline calcite (figure 2H). The porosity of this microfacies is

represented by vug and intercrystalline (figure 2I) porosity types. The slightly enrichment of the micrite matrix and low diversity of the faunal content in this microfacies reveal a quiet, open marine, shallow subtidal, depositional environment of this microfacies that correlated with the microfacies types in FZ7 of [23].

Molluscan echinoidal packstone

This carbonate microfacies type is recorded at the top part of the Matulla Formation. Allochems in Molluscan echinoidal packstone microfacies compose about 50 % of the rock and are represented by molluscan and echinoid fragments. Bivalve shall fragment have been recrystallized and formed of prismatic crystalline calcite while the echinoid fragments are characterized by overgrowth calcite cement. The outer surfaces of pelecypod fragments are dissolute and appear as irregular surfaces. These bioclastic grains are embedded in the micrite matrix. That is occasionally recrystallized into microcrystalline calcite cement. Porosity in this microfacies is common and represented by intercrystalline, channel (figure 2J), intercrystalline, and vug (figure 2K) porosity types. The enrichment of molluscan bioclastic grains as well as the micrite matrix reflects the deposition of this microfacies in a quiet, restricted shallow subtidal environment. This interpretation of depositional environment coincides with that of [23] to his FZ7 microfacies.

Diagenesis

Diagenetic alteration types are controlled by environment conditions after sedimentation stage (post-depositional environment) but alteration degree is depending on exposure duration [32].

Physical properties of the sedimentary rocks are affected by diagenesis operations and rock porosity increased with decreasing the depth of deposition (low overburden) while, tectonic influence reduced by lower geothermal gradient [33]. The main influences in the most diagenetic processes are primary mineralogical composition, environment of sedimentation and fluids flow nature. Contact zone is the place of diagenesis operation controlled by the presence of one or more phase such as sediments compositions, fluids type (saline or fresh) and air also, degree of temperature, and CO₂ content [34]. Three main types of diagenetic processes that appeared in the thin section under investigation are dolomitization, neomorphism and dissolution.

Dolomitization

Dolomitization is chemical substitution process takes place after sedimentation and cementation stage by which limestone (CaCO₃) changed to dolomite (CaMg (CO₃)₂), in the presence of magnesium-rich water volume by volume (figures 2A and B) [35]. The dolomitization process cause increasing in rock porosity due to relict dissolution during dolomitized limestone to great extra porosity [36].

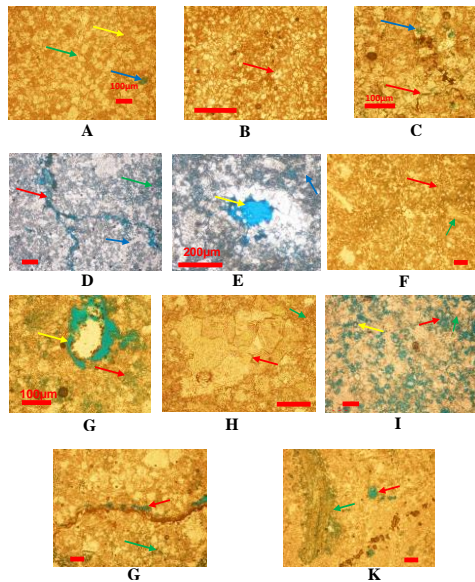


Figure 2. Photomicrographs of carbonate samples from microcopy show Dolostone microfacies including (A) Rhombs of dolomite crystals (green arrow), Vug porosity (blue arrow), micrite matrix (yellow arrow), sample No. 8. (B) Dolomite crystal zoned with iron oxide nuclei (red arrow), sample No. 10. (C) intercrystalline (red arrow), and intracrystalline (blue arrow) porosity, sample No. 15. Echinoidal foraminiferal grainstone microfacies including (D) intercrystalline (green arrow), channel porosity (red arrow), and Pelecypod shall fragments (blue arrow), sample No. 24. (E) Vug porosity (yellow arrow), and Pelecypod shall fragments (blue arrow), sample No. 29. Echinoidal foraminiferal packstone microfacies including (F) micrite matrix (red arrow) and Pelecypod shall fragments (green arrow), sample No. 41, (G) Vug (yellow arrow), and intercrystalline porosity (red arrow), sample No. 36. Echinoidal bioclastic Packstone/grainstone microfacies including (H) partially recrystallized micrite matrix to macro crystalline calcite cement (red arrow), (spary calcite) (Neomorphasam) and fauna fragments (green arrow), sample No. 53. (I) Vug (yellow arrow), and intercrystalline porosity (red arrow) and fauna fragments (green arrow), sample No. 44. Molluscan Echinoidal packstone microfacies including (J) intercrystalline (green arrow), and channel porosity (red arrow), sample No.83. (K) Intercrystalline (green arrow), and Vug porosity (red arrow), sample No. 85.

Neomorphism

The transformation of minerals (moist metamorphic process) into either crystalline or polymorphs structures identical to the original rock is called neomorphism [37]. Neomorphism take place in carbonate with two aspects includes wet recrystallization of cryptocrystalline calcite (micrite) to calcite or wet polymorphism is transformation of aragonite to calcite [38], in our study the micrite microfacies of carbonate is susceptible to diagenetic recrystallized into a macro-crystalline mosaic due to aggrading neomorphism (figures 2D, and E).

Dissolution

Carbonate grains and types of cement exhibit dissolution features [39, 40, and 41]. Dissolution is defined as a process of dissolving components, has great importance in chemical processes in carbonate rock causing selective leaching for unstable minerals

forming caverns, vugs and secondary pores leading to increasing in the effective and secondary porosity (figures 2E, and G).

Petrophysical Relationships

The petrophysical calculation and their relationships included average values and standard deviations were determined for all studied microfacies (Dolostone, Echinoidal foraminiferal grainstone, Echinoidal foraminiferal packstone, Echinoidal bioclastic packstone/grainstone, and Molluscan echinoidal packstone) which are compiled in Table (1). Petrophysical studies were used to determine the extent to which the petrophysical behavior was affected by the diagenetic events. Petrophysical data that was extracted revealed that they aren't homogeneous to a large extent, the non-homogeneous depended on rock type and their pore space distribution, mineralogical composition, fossils, clay content and size of crystal, [42]. The following is a discussion of the studied petrophysical behaviors.

Bulk density –Porosity

The relationships between the porosity and bulk density figure 3 was determined for all studied carbonate microfacies (Dolomitic packstone, Echinoidal foraminiferal grainstone, Echinoidal foraminiferal packstone, Echinoidal bioclastic packstone/grainstone, and Molluscan echinoidal packstone) are shown in Figure 3. The results gained from the porosity and bulk density relationships show excellent linear inverse shape, also show high and reliable coefficient of correlations (R^2) of values reached 0.91, 0.99, 0.98, 0.98, and 0.88, respectively, the linear shape show rock homogeneity due to the similarity in packing, fabric, grain shape and mineralogical composition. The bulk density is expected with great precision from porosity measurements. The relationships between the porosity and bulk density was calculated for all studied carbonate using the following equations:-

For Dolostone

$$\Phi = 1.01 - 0.37d_b \quad (10)$$

For Echinoidal foraminiferal grainstone

$$\Phi = 1.11 - 0.42d_b \quad (11)$$

For Echinoidal foraminiferal packstone

$$\Phi = 1.03 - 0.38d_b \quad (12)$$

For Echinoidal bioclastic packstone/grainstone

$$\Phi = 1.07 - 0.40d_b \quad (13)$$

For Molluscan Echinoidal packstone

$$\Phi = 0.97 - 0.36d_b \quad (14)$$

Porosity - Permeability

The permeability of rocks are defined as the ability of rock to conduct the fluids. Which this ability affected with many geological factors like as tortuosity, packing shape, size and roundness of the grain and pore space volume. The high porosity of the rocks does not reflect high permeability, some rocks contain low permeability high porosity such as Pumice stone and shale, also some carbonate rock contained micro fracture show high permeability and low porosity. The relationship cross plot of porosity and permeability of the studied carbonate rocks are

shown in figure 4 reveals directly proportional relationship appears in a power and indicate positive trend. Dolomitic packstone and Echinoidal foraminiferal packstone for carbonate rocks are very weak coefficient of correlations ($R^2 = 0.13$ and 0.19 respectively) and no relation for Echinoidal foraminiferal grainstone, Echinoidal bioclastic packstone/grainstone and Molluscan echinoidal packstone. Some samples of studied carbonate microfacies marked very weak relations between porosity and permeability not bake to the porosity factor only but may be as a result of increasing the fine particles or difference in tortuosity shape.

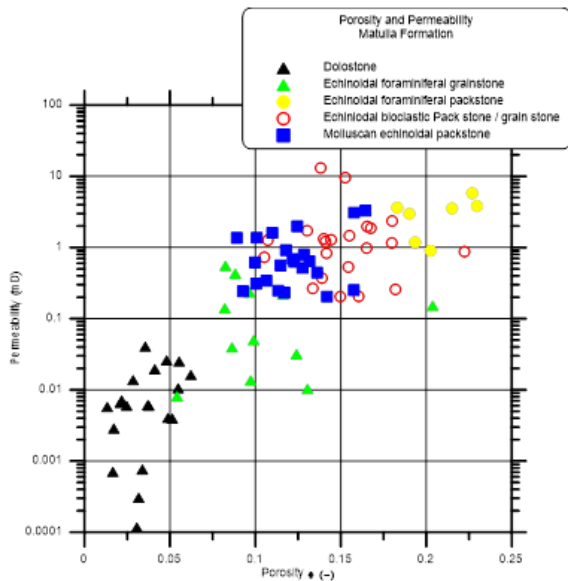


Figure 3: Permeability versus porosity for all samples.

Porosity - Reservoir quality index (RQI)

Porosity and logarithm reservoir quality index relationship is shown in figure 5 for all rock samples which, reveals $RQI < 1 \mu m$ for all carbonate samples indicated to poor reservoir quality. The porosity - RQI relationship for all microfacies is highly scattered characterized by a weak to the very weak coefficient of correlation.

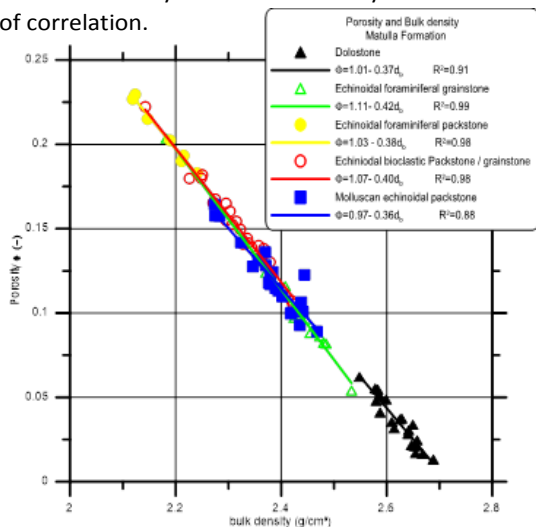


Figure 4: Porosity versus bulk density for all studied samples.

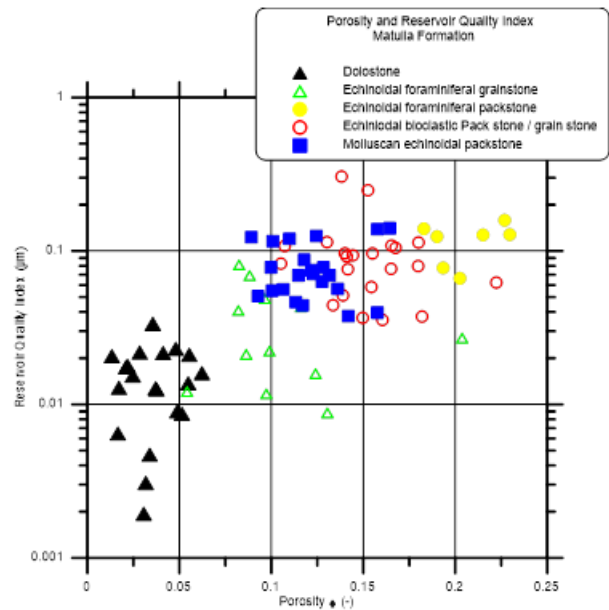


Figure 5: Reservoir quality index versus porosity for all samples.

Permeability - Reservoir quality index

Reservoir quality index was calculated using equation (5), a strong correlation is expected between permeability and RQI . The results values of reservoir quality index and permeability as in figure 6 are depended on permeability due to directly proportional relationships with high correlation coefficient $R^2 = (0.91, 0.95, 0.98, 0.95$ and $0.96)$ for Dolomitic packstone, Echinoidal foraminiferal grainstone, Echinoidal foraminiferal packstone, Echinoidal bioclastic packstone/grainstone, and Molluscan echinoidal packstone, microfacies carbonate samples, respectively. Permeability - Reservoir quality index relationships are calculated with following equations:

For Dolostone
 $RQI = [10]^{-0.87} * [K]^{0.45}$ (15)

For Echinoidal foraminiferal grainstone
 $RQI = [10]^{-1.02} * [K]^{0.49}$ (16)

For Echinoidal foraminiferal packstone
 $RQI = [10]^{-1.15} * [K]^{0.47}$ (17)

For Echinoidal bioclastic packstone/grainstone
 $RQI = [10]^{-1.09} * [K]^{0.50}$ (18)

For Molluscan Echinoidal packstone
 $RQI = [10]^{-1.05} * [K]^{0.48}$ (19)

The exponents of k are close to 0.5 as suggested by equation (5). Considering the weak variation in porosity within the studied microfacies, it becomes obvious that the RQI reflects mainly changes in permeability.

Porosity - Flow zone indicator (FZI, μm)

The relationship between porosity and flow zone indicator shown in figure 7 for the studied different types of microfacies carbonate samples, the Figure reveals shows the weak relationship between FZI values and porosity values for all microfacies.

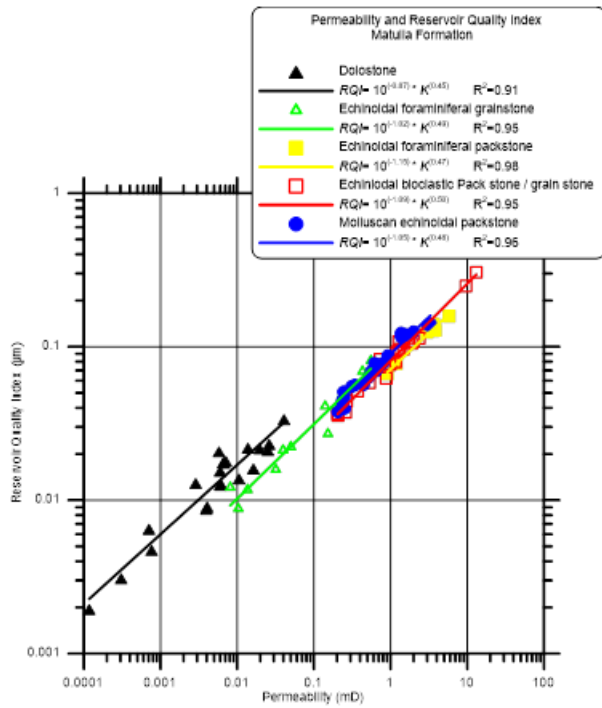


Figure 6: Reservoir quality index versus permeability for all samples.

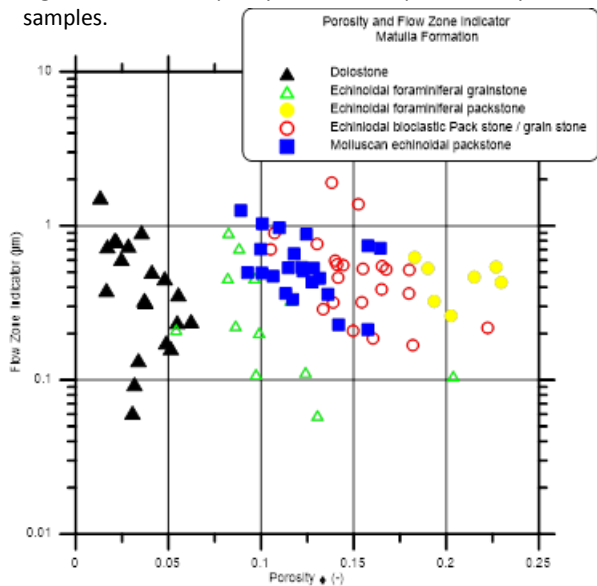


Figure 7: Flow zone indicator versus porosity for all samples.

Permeability - Flow zone indicator (FZI, μm)

The relationships between the permeability and flow zone indicator (FZI, μm) is shown in figure 8. Permeability and Flow zone indicator relationships are calculated with following equations:

For Dolostone

$$FZI = [10]^{-0.39} * [K]^{0.35} \quad (20)$$

For Echinoidal foraminiferal grainstone

$$FZI = [10]^{-0.10} * [K]^{0.45} \quad (21)$$

For Echinoidal foraminiferal packstone

$$FZI = [10]^{-0.53} * [K]^{0.40} \quad (22)$$

For Echinoidal bioclastic packstone/grainstone

$$FZI = [10]^{-0.34} * [K]^{0.49} \quad (23)$$

For Molluscan Echinoidal packstone

$$FZI = [10]^{-0.19} * [K]^{0.43} \quad (24)$$

From the previous relationships mentioned above, we conclude that the Flow zone indicator (FZI, μm) was affected with permeability values for all carbonate microfacies. The values of the correlation coefficient are $R^2 = (0.41 \text{ and } 0.62)$ for Dolomitic packstone and Echinoidal foraminiferal grainstone respectively and reliable coefficient of correlation (0.63 and 0.65,) for Echinoidal bioclastic packstone/grainstone and Molluscan Echinoidal packstone respectively and higher coefficient of correlation (0.79) for Echinoidal foraminiferal packstone. Considering the definition of FZI in equation (7), we find that the permeability directly affects the FZI. The exponents of k in equations (20-24) are similar to the exponents in equations (15-19) that show the relationships between k and RQI.

Hydraulic flow zone indicator

The Hydraulic Flow Unit (HFU) can be divided according to the core analysis data, [10]. From the core permeability and porosity measurements, the values of FZI, NPI, and RQI, for each core sample were calculated by Equations 5, 6, and 7.

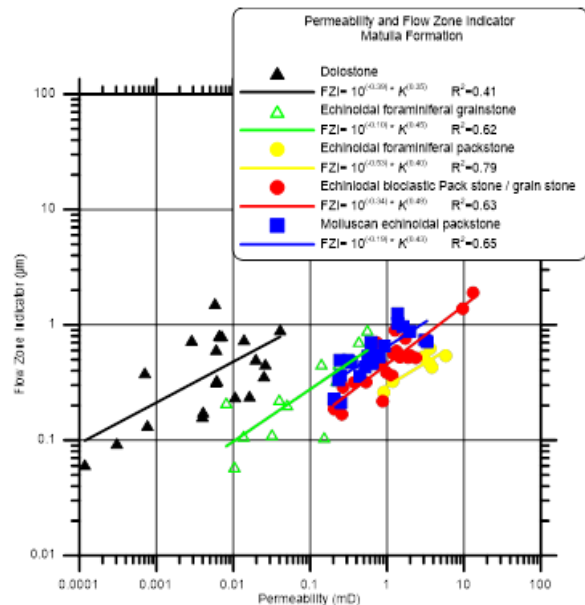


Figure 8: Flow zone indicator versus permeability for all samples.

Figure 9 show logarithmic plot of the relation between RQI versus NPI give straight line with unit slope, the value of flow zone indicator (FZI) determined when straight line intercept with y axis (NPI=1).

The studied carbonate samples divided into two hydraulic flow units by calculating the flow zone indicator from porosity and permeability measurements. The values of FZI was recorded from 0.06 to 1.91 μm at standard deviation equal 0.26 and mean value of 0.59 which infers poor reservoir quality, as shown in figure 10. Briefly, rock samples that contain pore filling, authigenic pore line, fine grains, and clays of pore bridging as well as poorly sorted particles exhibit high surface area and small value of FZI. But low surface area and high FZI exhibits with well-sorted and clean coarse grain size.

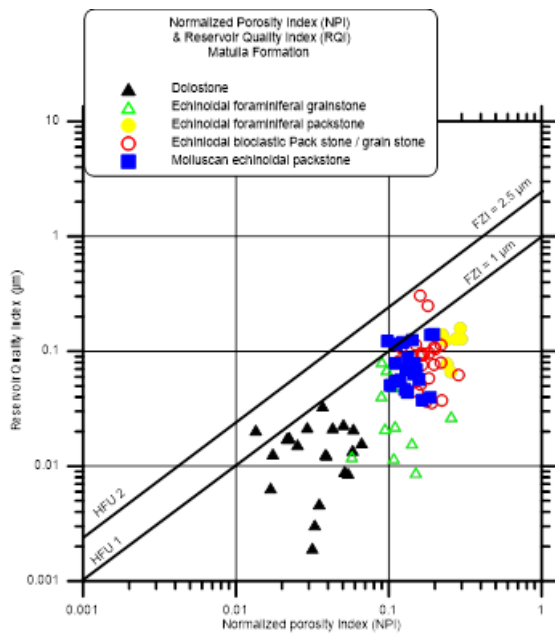


Figure 9: Reservoir quality index versus normalized porosity index for all samples.

The studied carbonate samples divided into two hydraulic flow units by calculating the flow zone indicator from porosity and permeability measurements. The values of FZI was recorded from 0.06 to 1.91 μm at standard deviation equal 0.26 and mean value of 0.59 which infers poor reservoir quality, as shown in figure 10. Briefly, rock samples that contain pore filling, authigenic pore line, fine grains, and clays of pore bridging as well as poorly sorted particles exhibit high surface area and small value of FZI. But low surface area and high FZI exhibits with well-sorted and clean coarse grain size. [43] model was used to derive the radius of the pore throat (R_{35}) by the data of core-porosity and permeability which, the estimated (R_{35}) is equal (0.01 to 2.66 μm) and it's plotted versus RQI, and FZI as shown in figures. 11 and 12. The Matulla Formation reservoir is comprised of micro to mesoporosity (0.01 μm < R_{35} ≤ 2 μm).

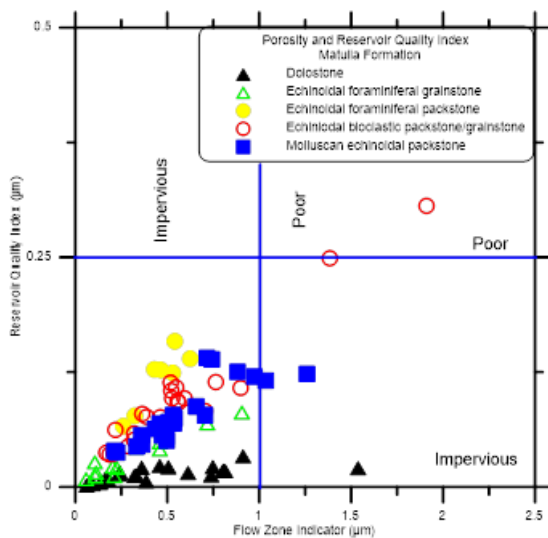


Figure. 10: Reservoir quality index versus flow zone indicator for all samples.

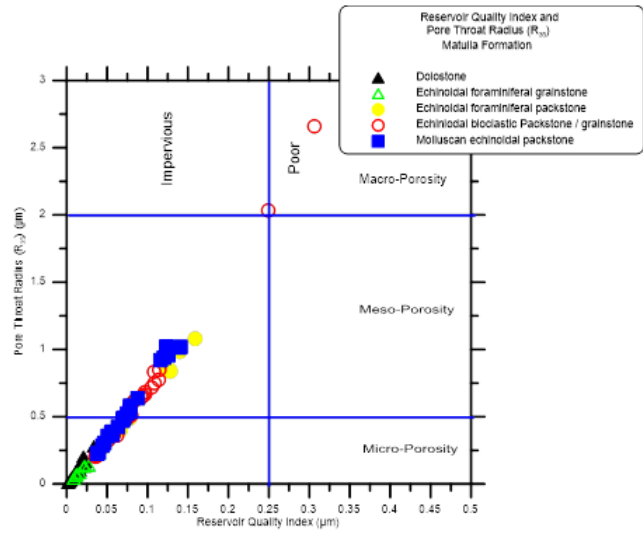


Figure. 11: Pore throat radius (R_{35}) versus reservoir quality index for all samples.

Reservoir characterization was determined according to the core samples analysis we conclude that the Matulla Formation intervals, due to their tight nature, are generally impervious and have poor flow potential and the hydraulic flow units of the carbonate microfacies divided into two unit of hydraulic flow (HFU1 and HFU2).

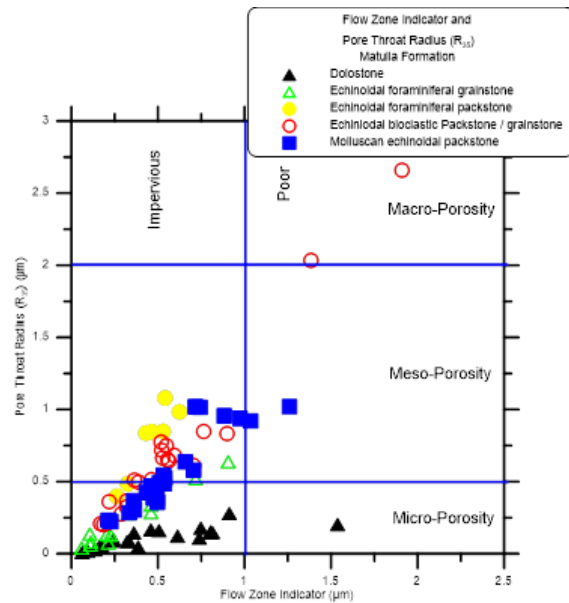


Figure 12: Pore throat radius (R_{35}) versus flow zone indicator for all samples.

Porosity - Formation factor

Cross plot relationship for all the studied samples shows a reverse trend due to increasing porosity with decreasing in formation factor as shown in figure 13. The relation between porosity and formation factor (F) is expressed by equation 25 are very important for outlining the water and hydrocarbon saturation of these formations during well logging processing and interpretation.

$$F = \frac{1.67}{\phi^{-1.27}} \tag{25}$$

Cementation factor (m) = 1.27 at a coefficient of determination $R^2 = 0.74$.

Table 1. Compilation of minimum, maximum, average values, and standard deviations of measured petrophysical parameters.

Facies	Parameters	Minimum	Maximum	Mean	Standard deviation
Dolostone	d_{bulk} (g/cm ³)	2.548	2.688	2.623	0.037
	d_{grain} (g/cm ³)	2.698	2.742	2.718	0.012
	Porosity Φ	0.013	0.062	0.035	0.014
	Permeability (mD)	0.0001	0.041	0.010	0.010
	Formation factor (F)	1208.40 0	7890.40 0	3559.4 57	2302.22 9
	RQI (μ m)	0.002	0.034	0.015	0.008
	NPI	0.013	0.066	0.036	0.015
	FZI (μ m)	0.062	1.538	0.497	0.361
	Echinoidal foraminiferal grainstone	d_{bulk} (g/cm ³)	2.182	2.533	2.421
d_{grain} (g/cm ³)		2.678	2.741	2.706	0.017
Porosity Φ		0.054	0.204	0.105	0.037
Permeability (mD)		0.008	0.554	0.157	0.178
Formation factor (F)		117.647	2761.50 0	1082.5 35	788.604
RQI (μ m)		0.009	0.081	0.034	0.024
NPI		0.057	0.256	0.119	0.050
FZI (μ m)		0.059	0.906	0.325	0.266
Echinoidal foraminiferal packstone	d_{bulk} (g/cm ³)	2.119	2.241	2.178	0.048
	d_{grain} (g/cm ³)	2.730	2.756	2.742	0.008
	Porosity Φ	0.183	0.230	0.206	0.018
	Permeability (mD)	0.906	5.804	3.126	1.674
	Formation factor (F)	189.600	415.600	321.25 3	76.716
	RQI (μ m)	0.066	0.159	0.118	0.033
	NPI	0.224	0.298	0.260	0.029
	FZI (μ m)	0.262	0.625	0.454	0.127
Echinoidal bioclastic packstone/grainstone	d_{bulk} (g/cm ³)	2.142	2.423	2.314	0.064
	d_{grain} (g/cm ³)	2.708	2.755	2.730	0.014
	Porosity Φ	0.105	0.222	0.152	0.026

	Permeability (mD)	0.205	13.147	1.987	3.147
	Formation factor (F)	189.600	2361.20 0	606.478	505.90 6
	RQI (μ m)	0.036	0.306	0.097	0.065
	NPI	0.118	0.286	0.181	0.037
	FZI (μ m)	0.168	1.910	0.564	0.407
Molluscan Echinoidal packstone	d_{bulk} (g/cm ³)	2.274	2.468	2.380	0.055
	d_{grain} (g/cm ³)	2.684	2.786	2.710	0.023
	Porosity Φ	0.089	0.164	0.122	0.021
	Permeability (mD)	0.205	3.309	0.928	0.882
	Formation factor (F)	312.500	2127.66 0	962.123	512.78 5
	RQI (μ m)	0.038	0.141	0.079	0.033
	NPI	0.098	0.197	0.139	0.027
	FZI (μ m)	0.212	1.260	0.588	0.264

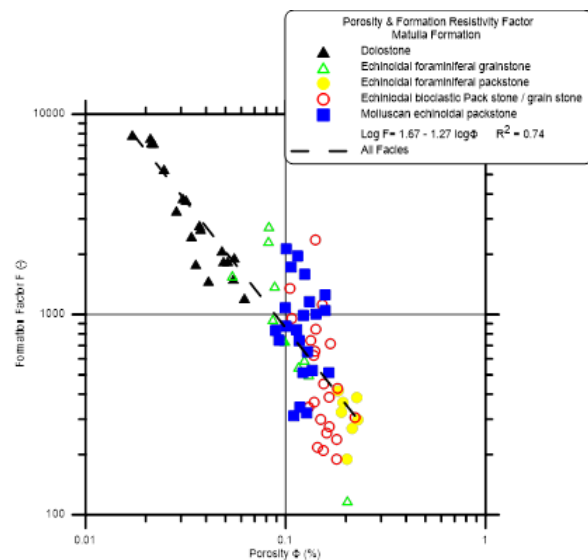


Figure 13: Formation resistivity factor versus porosity for all samples.

Permeability - Formation factor

The cross plot between formation factor and permeability, which is shown in figure 14, yields the following fitting equation considering all samples of this study:

$$k = [10]^{(4.22)} * [F]^{(-1.67)} \quad (26)$$

with a weak coefficient of determination $R^2 = 0.41$.

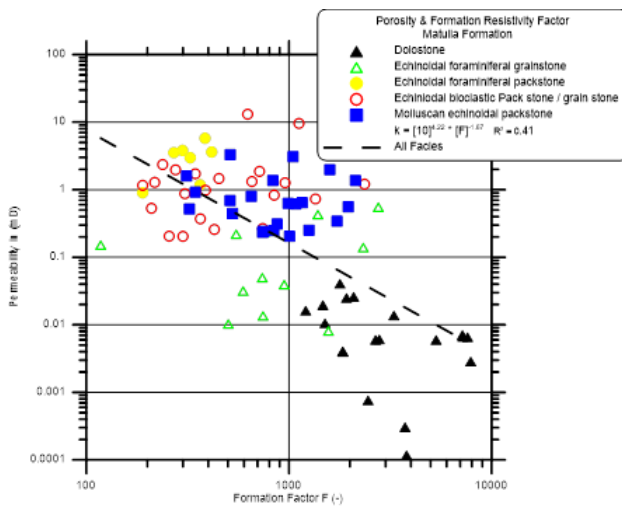


Figure 14: Formation resistivity factor versus permeability for all samples.

Conclusions

The results of the study aims to flash up at the microfacies and integration of reservoir properties that carried out on Matulla Formation of Upper Cretaceous incident at Gabal Libni included mineralogical composition, structure, texture and thin section examination, faunal content and which revealed that the Matulla Formation can be divided into five microfacies of carbonate, Dolostone, Echinoidal foraminiferal grainstone, Echinoidal foraminiferal packstone, Echinoidal bioclastic packstone/grainstone and Molluscan echinoidal packstone, also thin section examination of carbonate samples revealed that most of the carbonate samples are tight. The density affected by porosity that commonly reduced by cementation, iron oxide, and clay content. The enrichment of the micrite matrix and the depletion of the bioclastic grains, with exception of few pelecypod reflect the deposition in quiet, restricted shallow subtidal environment as well as the initial cryptocrystalline calcite matrix and low diversity of the faunal content can be reflect quiet open marine, also the enrichment of molluscan bioclastic grains reflect the deposition in quiet, restricted shallow subtidal environment. Several intersecting diagrams of cross plot that have been drawn and can be successfully used to differentiate limestone microfacies. The results of the studied samples reflect the reservoir quality of fair to bad due to poor permeability and low porosity values, the stronger decrease in porosity and permeability is

observed for the Dolomitic Packstone microfacies. The relevant cross plot of large scatter indicates that the diagenesis, matrix, clay pore filling, and iron oxides cause a decrease in porosity and permeability. The FZI for all carbonate microfacies ranged from 0.06 to 1.91 μm , the hydraulic flow units of the studied carbonate represent by two hydraulic flow units (HFU1 and HFU2) depending on the values of flow zone indicator (FZI). The permeability of individual samples is dominated by the flow zone index (FZI) and reservoir quality index (RQI) values. The reservoir quality index (RQI) ranges from 0.002 to 0.306 μm compensation by the average values of permeability 1.05 mD, this reveals that the reservoir quality of carbonate rock samples are very low. Changes in porosity indicate only a minor influence on these parameters. Considering the FZI for all microfacies classification they are classified as infers impermeable for weak hydraulic flow units. The estimated pore throat radius (R35) ranges from (0.01 to 2.66 μm) for Matulla Formation reservoir is comprised of micro to mesoporosity (0.01 $\mu\text{m} < R35 \leq 2 \mu\text{m}$). Depending on core reservoir characterization, we conclude that the Matulla Formation intervals, due to their tight nature, are generally impervious and have poor flow potential. The Archie's law between formation factor and porosity is confirmed by our data set and the resulting constant factor $a = 1.67$ and cementation factors is $m = 1.27$ for all studied microfacies.

Funding sources

"This research received no external funding".

Conflicts of interest

"There are no conflicts to declare".

Acknowledgements

Authors express their sincere gratitude to (Editor-in-Chief) the Journal of Petroleum and Mining Engineering and the reviewers for their constructive reviews which benefited our work. Interpretation presented in this paper is solely of the authors and does not necessarily reflect their respective organizations.

References

- [1] Carman PC, Fluid flow through granular beds. *Trans Inst Chem Eng* 15: (1937) 150–166.
- [2] Timur A., An investigation of permeability, porosity, and residual water saturation relationships. SPWLA 9th annual logging symposium, Society of Petrophysicists and Well-Log Analysts, 1968.
- [3] Scheidegger A., The physics of flow through porous media. University of Toronto, Toronto Press, (1974) p353.
- [4] Herron M., Estimating of intrinsic permeability of elastic sediments from geochemical data. *Trans. SPWLA.* (1987) P. 6.
- [5] Adler P, Jacquin CG, Quiblier J., Flow in simulated porous media. *Int J Multiph Flow* 16: (1990) 691–712.
- [6] Schon JH., Handbook of geophysical exploration: fundamentals and principles of petrophysics. Pergamon, Seismic Exploration. Physical Properties of Rocks, 1996
- [7] Tiab, D., Donaldson, E.C., *Petrophysics: theory and practice of measuring reservoir rock and fluid transport properties.* Gulf professional publishing, 2015.
- [8] Kassab MA, Teama MA., Hydraulic flow unit and microfacies analysis integrated study for reservoir characterization: a case study of Middle Jurassic rocks at Khashm El-Galala, Gulf of Suez Egypt. *Arab J Geosci* 11 (12): (2018) 294.
- [9] Farouk A, Sen S, Ganguli SS, Abuseda H, Debnath A., Petrophysical assessment and permeability modeling utilizing core data and machine learning approaches – a study from the Badr El Din-1 field, Egypt. *Mar Pet Geol* 133, (2021) 105265.
- [10] Amaefule, J.O., Altunbay, M., Tiab, D., Kersey, D.G., Keelan, D.K., Enhanced reservoir description: using core and log data to identify hydraulic (flow) units and predict permeability in uncored intervals/wells, SPE annual technical conference and exhibition, Society of Petroleum Engineers, 1993.
- [11] Said, R., *The Geology of Egypt*, 734 p. Balkema, Rotterdam, 1990.
- [12] Bartov, Y., Steinitz, G., The Judea and Mount Scopus groups in the Negev and Sinai with trend surface analysis of the thickness data. *Isr. J. Earth Sci.* 61 (1977) 119 – 148.
- [13] Shaha, J., The Syrian arc system: an overview. *Palaeogeogr. Palaeoclimatol. Palaeoecol.* 112 (1994) 125–142
- [14] Tawadros, E.E., *Geology of Egypt and Libya.* Balkema, Rotterdam, (2001) 468.
- [15] El-Fawal, F., Sadek, A., Hassan, H.F., Sequence architecture and platform evolution of the Paleogene rocks in Sinai, Egypt. *GRMENA*, 1, (2005) 67-105.
- [16] Hancock, J.M., Sea –level changes around the Cenomanian-Turonian boundary. *Cretaceous Res. V.* 14 (1993) 553–562.
- [17] Haq, B.U., Hardenbol, J., Vail, P.R., *Mesozoic and Cenozoic chronostratigraphy and eustatic cycles* 1988.
- [18] Jenkins, D.A., North and central Sinai. In: Said, R. (Ed.), *The Geology of Egypt.* A.A. Balkema, Pub., Rotterdam (1990) 361 – 380 (734 pp).
- [19] Kusky, T.M., El-Baz, F., Structural and tectonic evolution of the Sinai Peninsula, using Landsat data: implications for ground water exploration. *Egypt. J. Remote Sens.* 1, (1999) 69 – 100.
- [20] Dickson JAD, A modified staining technique for carbonates thin section. *Nature* 205 (1965) 587.
- [21] Choquette PW, Pray LC., Geologic nomenclature and classification of porosity in sedimentary carbonates. *AAPG Bull* 54: (1970) 207 – 250.
- [22] Dunham RJ., Classification of carbonate rocks according to depositional textures. In: Ham WE (ed), *Classification of carbonate rocks*, Vol. 1. American Association Petroleum Geologists Memoir (1962) 108 – 121.
- [23] Wilson JL., Carbonate facies in geological history. Springer-Verlag, Berlin, (1975) p 471.
- [24] Flügel E., *Microfacies of carbonate rocks, analysis, interpretation and application*, 2nd Edn. Springer-Verlag, Berlin, (2004) p 984.
- [25] Wyllie, M., Spangler, M., Application of electrical resistivity measurements to problem of fluid flow in porous media. *AAPG Bulletin* 36 (1952) 359 - 403.
- [26] El Sayed, A.M.A., Geological and petrophysical studies for the Algyo-2 reservoir evaluation, Algyo oil and gas field, Hungary. Ph. D. thesis, Hung. Acad. Sci., Budapest (1981) 166.
- [27] Glover, P., What is the cementation exponent? A new interpretation. *The Leading Edge* 28 (2009) 82 - 85.
- [28] Abuseda, H., Weller, A., Sattler, C.-D., Debschütz, W., Petrographical and petrophysical investigations of upper cretaceous sandstones of the South West Sennan field, Western Desert, Egypt. *Arabian Journal of Geosciences* 9 (2016) 12.
- [29] Archie, G.E., The electrical resistivity log as an aid in determining some reservoir characteristics. *Petroleum Technology* 1 (1942) 54 – 62.
- [30] Wyllie, M., Gregory, A., Formation factors of unconsolidated porous media: Influence of particle shape and effect of cementation. *Journal of petroleum technology* 5 (1953) 103 - 110.
- [31] Revil, A., Cathles Iii, L., Permeability of shaly sands. *Water Resources Research* 35 (1999) 651 - 662.
- [32] Purdy, E.G., "Carbonate diagenesis". *An environmental Survey*, *Geol. Roman* 7 (1968) 183 - 228.
- [33] El-Verhol, A., and Groniles, G., Diagenetic and sedimentology explanation for high seismic sediment, Sualbord Region. *A.A.P.G., Bull.*, Vol. 65/1 (1981) 145 - 153.
- [34] Khalial, M.H., Petrology and geochemistry of the Turonian sedimentary sequence in Southern Sinai, Egypt. Ph.D. Theses. Al- Azhar Univ., Cairo, Egypt (2004) p. 274.
- [35] Zenger, D.H., Syntaxial calcite borders on dolomite crystal. *Little Falls, Jour. Sed. Petrol.*, Vol. 43 (1973) 118 - 124.
- [36] Tucker, E.M., *Sedimentary petrology an introduction to the origin of sedimentary rocks.* Department of Geological Sciences, University of Durham, Blackwell publications, 3rd ed. (2001) 62 - 65.
- [37] Folk, R.L., Some aspects of recrystallization in ancient limestone. In. (L.C. Pray and R.C. Murray Eds.) *Dolomitization and limestone diagenesis.* Soc. Econ. Paleont. Min. Spec. Publ. (13) (1965) 1 - 48.
- [38] Priezbindowski, D.R., Burial cementation is it important? A case study, Stuart City Treend, South-Central Texas. In: N. Schneidermann and P.M. Harris

- (eds.), Carbonate cement. SEPM spec. Pub. No. 36 (1985) 241 - 264.
- [39] Montgomery, S.L., and Dixon, W.H., New depositional model improves outlook for clear Fork infill drilling: Oil and Gas Journal, V.96 (1998) 94 - 98.
- [40] Pratt, B.R., Oceanography, bathymetry and syn-depositional tectonics of a Precambrian intracratonic basin: integrating sediments, storms, earthquakes and tsunamis in the Belt Super-group (Helena Formation, ca. 1.45 Ga), Western North America: Sedimentary Geology, Vol. 141 (2001) 371 - 394.
- [41] El-Hariri, T.Y., Mousa, A.S. and Ibrahim, G. El-Din., Digenetic processes, geochemistry and petrophysical properties of the Upper Cretaceous Matulla and Thelmet formations at Wadi El Ghaib, South-eastern Sinai, Egypt. Aust. J. of Bas. And Appl. Sci., 1(4). (2007b) 487 - 496.
- [42] B.S. Nabawy, Impacts of Dolomitization on the Petrophysical Properties of El-Halal Formation, North Sinai, Egypt, Arabian Journal of Geosciences, 6 (2013) 373.
- [43] Kolodzie Jr., S., Analysis of pore throat size and use of the Waxman-Smiths equation to determine OOIP in Spindle field, Colorado: Society of Petroleum Engineers 55th Annual Fall Technical Conference, SPE Paper No. 9382 (1980) 10 p.